Journal Pre-proof

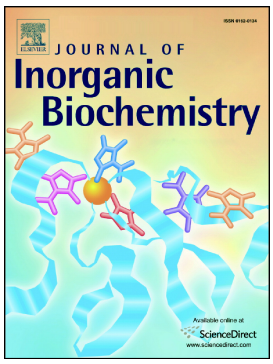


# Stabilization of an intermolecular RNA triplex by two novel binders Lys- and Arg-rich Ru(II) polypyridyl metallopeptides

Juan Zhu, Fangfang Wang, Xiaohua Liu, Lifeng Tan

PII: S0162-0134(20)30199-9

DOI: https://doi.org/10.1016/j.jinorgbio.2020.111171

Reference: JIB 111171

To appear in: *Journal of Inorganic Biochemistry*

Received date: 17 March 2020

Revised date: 25 June 2020

Accepted date: 25 June 2020

Please cite this article as: J. Zhu, F. Wang, X. Liu, et al., Stabilization of an intermolecular RNA triplex by two novel binders Lys- and Arg-rich Ru(II) polypyridyl metallopeptides, *Journal of Inorganic Biochemistry* (2020), https://doi.org/10.1016/j.jinorgbio.2020.111171

**Manuscript Number:** ***JINORGBIO-D-20-00105R1***

# Stabilization of an intermolecular RNA triplex by two novel binders Lys- and Arg-rich Ru(II) polypyridyl metallopeptides

Juan Zhu,[a] Fangfang Wang,[a] Xiaohua Liu,[b] Lifeng Tan[*c,d]

[a] *College of Chemistry, Xiangtan University, Xiangtan 411105, Peoples Republic of China*

[b] *Academic Affairs Office, Xiangtan University, Xiangtan 411105, Peoples Republic of China*

[c] *Key Lab of Environment-friendly Chemistry and Application in Ministry of Education, Xiangtan University, Xiangtan 411105, Peoples Republic of China. E-mail address: lfwyxh@yeah.net; Tel: +86 731 58293997*

[d] *Key Laboratory for Green Organic Synthesis and Application of Hunan Province, Xiangtan University, Xiangtan 411105, Peoples Republic of China*

**ABSTRACT**

In this work, using $[Ru(bpy)_2(pip)]^{2+}$ (bpy = 2,2′ -bipyridine, pip = 2-phenyl-1*H*-imidazo[4,5-*f*]-[1,10]-phenanthroline) as chromophores and neutral amino acid glycine as spacers, two novel Arg- and Lys-rich Ru(II) polypyridyl metallopeptides as an intermolecular triplex RNA stabilizers, namely $[Ru(bpy)_2(pic\text{-}Lys_2\text{-}Gly\text{-}Lys_2\text{-}Gly\text{-}Lys_2)]^{8+}$ (Ru**1**; pic = 2-(4-carboxy-phenyl)imidazo-[4,5-*f*][1,10]phenanthroline, Gly = glycine, Lys = lysine) and $[Ru(bpy)_2(pic\text{-}Arg_2\text{-}Gly\text{-}Arg_2\text{-}Gly\text{-}Arg_2)]^{8+}$ (Ru**2**; Arg = arginine), have been synthesized and characterized. The binding properties of Ru**1** and Ru**2** with poly(U)•poly(A)*poly(U) triplex have been studied by by UV–Vis spectroscopy, fluorescence spectroscopy, viscosity measurements as well as circular dichroism and thermal denaturation. The obtained results suggest that attaching cationic peptides to a Ru(II) polypyridyl complex can obviously enhance the triplex stabilization. Considering the structure natures of Ru**1** and Ru**2**, conceivably besides electrostatic interaction, the forces stabilizing the triplex should also involve hydrophobic interaction and hydrogen binding. Compared with the Lys-rich metallopeptide (Ru**1**), however, the third-strand stabilizating effect of the Arg-rich one (Ru**2**) is slightly more marked, which may be due to differences in the interactions of arginine and lysine residues with the third strand of the triplex. The results obtained here may be useful for understanding the interaction of triplex RNA poly(U)·poly(A)*poly(U) with small molecule, particularly ruthenium(II) complexes.

***Keywords***: Ru(II) polypyrdiyl metallopeptide; RNA triplex; Third-strand stabilization

## 1. Introduction

Structure diversities presented in RNA molecules make them play essential roles in many biological processes [1]. Evidence indicates that intermolecular RNA triplexes are implemented to mediate catalysis during telomere synthesis and RNA splicing, bind to ligands and ions so that metabolite-sensing riboswitches can regulate gene expression, and provide a clever strategy to protect the 3' end of RNA from degradation [1]. However, the thermal stabilization of RNA triplexes is a key factor for applying the triplex concept under physiological conditions, the reason for this is that the stabilization of a Hoogsteen strand (third-strand) is much lower than that of the Watson-Crick base-paired duplex of RNA triplexes [2]. For example, the first and second melting temperatures for poly(U)•poly(A)*poly(U) (where • denotes the Watson–Crick base pairing and * denotes the Hoogsteen base pairing) triplex usually occurr at *ca.* 35 and 45 °C, respectively [3]. Thus, the low thermal stabilization of the third strand limits their practical applications under physiological conditions [2]. In this regard, small molecules able to stabilize RNA triplexes are in great demands.

Much effort in recent years has been directed to design of small molecules with diverse structure traits to improve the triplex stabilization [4]. Studies suggested that the triplex stabilization could be increased by the action of intercalators in particular when covalently linked to the third strand, [5,6] while intercalators not covalently linked could either stabilize or destabilize the triplex [4f], reflecting that structural features of small molecules influencing the triplex stabilization were very complicated. Although many small molecules with different structures have been synthesized to stabilize an intermolecular RNA triplex in recent years, small molecules used to stabilize RNA triplexes are currently concentrated in small organic compounds [5]. Therefore, there is relatively

little information on an RNA triplex stabilized by metal complexes at present [7]. Our laboratory recently has designed a handful of Ru(II) polypyridyl complexes as RNA triplex stabilizers [8]. Primary studies have shown that subtle modifications of either the intercalative or ancillary ligands surrounding the metal centre may significantly affect the triplex stabilization, which further underlines the complexity of the RNA–metal complex system. To determine the factors effect on the triplex stabilization of small molecules, studies on Ru(II) complexes with different shapes and electronic properties affecting the binding behaviors are very necessary.

To efficiently enhance the triplex stabilization, the typical structure characteristics of main lingands in Ru(II) complexes had better be crescent shaped [9], whereas which usually requires demanding synthetic procedures and hence limits the efficient access to further structural modification. In this regard, we assume that: 1) a promising alternative would be the decoration of triple-helical binders with cationic peptide sequences to modify their physicochemical properties in a more predictable and synthetically-accessible approach; 2) the triplex stabilization could be remarkably increased by cationic amino acid residues of Ru(II) polypyridyl metallopeptides effectively binding to and neutralizing phosphate groups of the triplex and increasing electrostatic attraction to the negatively charged nucleic acid. Furthermore, we note that lysine- or arginine-rich metallopeptides, capable of binding unique nucleic acid structures have increased interest in the development of small molecule binders in recent years [10]. For example, the first study about the effect of the presence of an oligoarginine functionalization in the recognition of G-quadruplexes reflects that the appending of a octaarginine tail to a Ru-dppz complex can significantly increase the stabilization of different G-quadruplexes sequences [11], which reflect that this approach has great potential in modifications of DNA binders based on Ru(II) polypyridyl complexes. Following our interest in improving the

triplex stabilization, hence we decide to explore the effect of Ru(II) polypyridyl complexes modified with basic oligopeptides on the binding properties.

Given that Ru(II) complex $[Ru(bpy)_2(pip)]^{2+}$ (bpy = 2.2'-bipyridine, pip = 2-phenyl-1*H*-imidazo[4,5-*f*][1,10]phenanthroline) is able to insert the aromatic ligand pip into double helix DNA [12] and subsequently many analogues by modifying pip have been developed as excellent DNA binding agents [13], we recently studied the binding properties of this complex with poly(U)•poly(A)*poly(U) triplex. The obtained results indicated that this complex showed a modest triplex stabilizing effect without affecting the stabilization of the Watson–Crick base pairing strand of the triplex [14]. To effectively improve the triplex stabilization, we will focus our attention on $[Ru(bpy)_2(pip)]^{2+}$ modified with basic peptides and hope that basic peptide-bridged Ru(II) polypyridyl complexes may open new perspectives for designing RNA triplex stabilizers.

In this work, using $[Ru(bpy)_2(pip)]^{2+}$ as chromophores and neutral amino acid glycine as spacers, two Arg- and Lys-rich Ru(II) polypyridyl metallopeptides (Scheme 1) as the RNA poly(U)•poly(A)*poly(U) triplex stabilizers, namely $[Ru(bpy)_2(pic\text{-}Lys_2\text{-}Gly\text{-}Lys_2\text{-}Gly\text{-}Lys_2)]^{8+}$ (Ru**1**; pic = 2-(4-carboxy-phenyl)imidazo[4,5-*f*][1,10]phenanthroline, Gly = glycine, Lys = lysine) and $[Ru(bpy)_2(pic\text{-}Arg_2\text{-}Gly\text{-}Arg_2\text{-}Gly\text{-}Arg_2)]^{8+}$ (Ru**2**; Arg = arginine), have been synthesized and characterized. Binding properties of Ru**1** and Ru**2** with the RNA triplex have been studied by spectrophotometric technologies and viscosity measurements.

## 2. Experimental section

*2.1. Materials*

Compounds 1,10-phenanthroline-5,6-dinone and *cis*-[$Ru(bpy)_2Cl_2$]•$2H_2O$ (bpy = 2,2′-bipyridine) [15] were prepared according to literature procedures. 4-Carboxybenzaldehyde was obtained from Sigma-Aldrich Corporation (St. Louis, MO, USA). Two peptides, pip -CO-$Lys_2$-Gly-$Lys_2$-Gly-$Lys_2$ and pip-CO-$Arg_2$-Gly-$Arg_2$-Gly-$Arg_2$ were synthesized by Shanghai Co. Ltd (Shanghai, China) except the starting material of pip-$CO_2H$ provided by our laboratory. The two peptides, were purified by high-performance liquid chromatography, and their purities (> 90%) and mass were confirmed by electrospray ionization mass spectrometry. Polynucleotide samples of double-stranded poly(A)⋆ poly(U) and single-strand poly(U) were obtained from Sigma-Aldrich Corporation (St. Louis, MO, USA) and were used as received. Formation of the triplex poly(U)•poly(A)⋆ poly(U) was carried out as reported earlier [3]. The concentrations of poly(U)•poly(A)⋆ poly(U) and poly(A)•poly(U) were determined optically using molar extinction coeffcients, $\varepsilon$ ($M^{-1}$ $cm^{-1}$) reported in the literature [16].

*2.2. Physical measurement*

Microanalyses (C, H and N) were carried out on a Perkin-Elmer 240Q elemental analyzer. $^1$H NMR (NMR = nuclear magnetic resonance) spectra were collected on an Avance-400 spectrometer with DMSO-$d_6$ (DMSO = dimethylsulfoxide) as solvent at room temperature and TMS (TMS = tetramethylsilane) as the internal standard. Mass spectrometry was performed on an Autoflex III™ Maldi-TOF-MS (Maldi-TOF-MS = matrix assisted laser desorption ionization time-of-flight mass spectrometry) (Bruker) using $CH_3CN$ as the mobile phase. UV-visible (UV-vis) spectra were recorded on a Agilent spectrum Cary 100 spectrophotometer, and emission spectra were recorded on PTI Qm400 luminescence spectrometer at room temperature. Optical rotations were measured using a Perkin-Elmer (Boston, MA) 341 LC polarimeter equipped with mercury lamp. Circular

dichroic (CD) spectra were measured on a JASCO-810 spectropolarimeter.

*2.3 Synthesis of 2-(4-carboxyphenyl)imidazo[4,5-f][1,10]phenanthroline (pip-$CO_2H$)*

A mixture of ammonium acetate (3.5 g, 45 mmol), 4-carboxybenzaldehyde (150 mg, 1 mmol) 1,10-phenanthroline-5,6-dione (210 mg, 1 mmol) and glacial acetic acid (40 mL) was refluxed for 4h under argon atmosphere. After cooled to room temperature, diluted with amount of water (30 mL) and neutralized with concentrated aqueous ammonia. The resulting orange solution was removed to give an orange powder, which was washed with amounts of water and dried under vacuum. Yield: 255 mg, 75%. MALDI-TOF-MS (DMSO, m/*z*): 341.1 ($[M+1]^+$).

*2.4 Synthesis of [Ru(bpy)$_2$(pic-Lys$_2$-Gly-Lys$_2$-Gly-Lys$_2$)]Cl$_8$ (Ru**1**)*

*Cis*-$[Ru(bpy)_2Cl_2]\cdot 2H_2O$ (15 mg, 0.03 mol ) and pic-$Lys_2$-Gly-$Lys_2$-Gly-$Lys_2$ (35 mg, 0.03 mol ) were heated to reflux in 10 mL of an ethanol/$H_2O$ (8:2) mixture under argon for 9 h with vigorous stirring. The red solution was cooled to room temperature and then treated with a saturated aqueous solution of LiCl. After that, the dark red crude product was obtained by vacuum-rotary evaporation and dried under vacuum. The product was purified on a neutral alumina column with MeCN-toluene (1:1, v/v) as eluant. Yield: 34 mg, 70%. MALDI-TOF-MS (DMSO, m/*z*): 1635.77 ($[M-8Cl^--7H^+]^+$), 818.44 ($[M-8Cl^--6H^+]^{2+}$), 545.95 ($[M-8Cl^--5H^+]^{3+}$), 409.71 ($[M-8Cl^--4H^+]^{4+}$). Anal. Calc. For $C_{80}H_{112}N_{22}O_{10}Cl_8Ru$: C 49.87, H 5.86, N 16.00; found: C 49.86, H 5.89, N 15.98. UV-Vis $\lambda_{max}$/nm ($\varepsilon$/$M^{-1}$ $cm^{-1}$, DMSO): 459 (13300), 291 (74700). $^1$H NMR (400 MHz, DMSO-$d_6$): $\delta$ 15.25 (s, 1H), 9.44 (s, 2H), 9.11 (s, 2H). 8.88 (dd, $J_1$ = 8.0 Hz, $J_2$ = 15.6 Hz, 4H), 8.74 (d, $J$ = 7.2 Hz, 1H), 8.56 (d, $J$ = 8.0 Hz, 2H), 8.29 (d, $J$ = 7.2 Hz, 8H), 8.30–8.13 (m, 2H); 8.13– 8.04 (m, 4H), 7.87 (t, $J_1$

= 17.2 Hz, $J_2$ = 20.0 Hz, 16H), 7.61 (d, $J$ = 10.8 Hz, 4H), 7.35 (t, $J_1$= 6.8 Hz, $J_2$ = 6.4 Hz, 2H), 4.19 (t, $J_1$ = 30.0 Hz, $J_2$ = 37.6 Hz, 6H), 3.91–3.64 (m, 4H), 2.77 (s, 12H); 1.81-1.23 (m, 36H).

*2.5 Synthesis of [Ru(bpy)$_2$(pic-Arg$_2$-Gly-Arg$_2$-Gly-Arg$_2$)]Cl$_8$ (Ru**2**)*

Synthesis of [Ru(bpy)$_2$(pic-Arg$_2$-Gly-Arg$_2$-Gly-Arg$_2$)]$^{2+}$ was performed similar to that described for Ru**1**, with pip-CO-Arg$_2$-Gly-Arg$_2$-Gly-Arg$_2$ instead of pic-Lys$_2$-Gly-Lys$_2$-Gly-Lys$_2$. Yield: 39 mg, 72%. MALDI-TOF-MS (DMSO, m/*z*): 1804.10 ([M-8Cl$^-$-7H$^+$]$^+$), 902.56 ([M-8Cl$^-$-6H$^+$]$^{2+}$), 602.04 ([M-8Cl$^-$-5H$^+$]$^{3+}$), 481.79 ([M-8Cl$^-$-4H$^+$]$^{4+}$). For $C_{80}H_{112}N_{34}O_{10}Cl_8Ru$: C 45.87, H 5.39, N 22.74; found: C 45.85, H 5.47, N 22.73. UV-Vis $\lambda_{max}$/nm ($\varepsilon$/M$^{-1}$cm$^{-1}$, DMSO): 459 (13500), 291 (77000). $^1$H NMR (400 MHz, DMSO-$d_6$): δ 10.03 (d, $J$ = 6.4 Hz, 2H); 9.52 (d, $J$ = 6.0 Hz, 2H); 8.88 (dd, $J_1$ = 8.4, $J_2$ = 15.6 Hz, 4H); 8.79 (d, $J$ = 7.2 Hz, 1H); 8.60 (d, $J$ = 8.0 Hz, 2H); 8.38 (d, $J$ = 7.6 Hz, 8H ); 8.27–8.04 (m, 10H); 7.94 (dd, $J_1$ = 5.2, $J_2$ = 8.4 Hz, 2H); 7.85 (t, $J_1$= 5.2H, $J_2$ = 8.4Hz, 2H); 7.77 (s, 2H); 7.60 (dd, $J_1$ = 4.8 Hz, $J_2$ = 12.8 Hz, 4H); 7.35 (t, $J_1$ = $J_2$ = 6.4 Hz, 2H); 7.05 (s, 12H ); 4.30 (d, $J$ = 30.8 Hz, 6H); 3.89-3.69 (m, 4H); 3.10 (s, 12H); 2.04-1.42 (m, 42H).

*2.6 Electronic Absorption Spectral studies*

UV−vis spectra were collected using an Agilent spectrum Cary 100 spectrophotometer at 20 °C. A typical titration of each metal complex in phosphate buffer was performed by fixing the metal complex concentration, to which the RNA triplex stock solution is gradually added up to saturation. After each addition, the solution should be mixed evenly and allowed to re-equilibrate for at least 3 min before recording the absorption spectra. the intrinsic binding constants ($K_b$) and the binding sites (*s*) are determined the changes of MLCT (MLCT = metal to ligand charge transfer) bands by

using the following equation [17]:

$$\frac{\varepsilon_a - \varepsilon_f}{\varepsilon_b - \varepsilon_f} = \frac{b - \sqrt{(b^2 - 2K_b^2 C_t [RNA]/s}}{2K_b C_t} \qquad (1a)$$

$$b = \frac{1 + K_b C_t + K_b [RNA]}{2s} \qquad (1b)$$

where [RNA] is the concentration of poly(U)•poly(A)*poly(U) in the nucleotide phosphate and $\varepsilon_a$, $\varepsilon_f$, and $\varepsilon_b$, respectively, are the apparent, free, and bound metal complex extinction coefficients. $K_b$ is the equilibrium binding constant in $M^{-1}$, $C_t$ is the total metal complex concentration, and $s$ is the binding site size in base pairs of Ru(II) complexes interacting with the triplex.

*2.7 Luminescence Titration with the RNA Triplex*

Luminescence titrations was carried out a PTI Qm400 luminescence spectrometer at 20 °C, and a dilute solution of Ru**1** or Ru**2** (2 μM) in phosphate buffer was excited at 470 nm. After each addition of the RNA triplex, the solution was mixed evenly and allowed to re-equilibrate for at least 3 min before recording the curve.

*2.8 Conformational aspects of the binding*

Circular dichroic spectrum of the RNA triplex in the absence and presence of each metal complex was performed with a Jasco-810 spectropolarimeter at 20 °C. After each addition of the metal complex, the solution was mixed evenly and allowed to re-equilibrate for at least 5 min before recording the CD spectra. Each spectrum was averaged from three successive accumulations and was baseline-corrected, smoothed, and normalized to nucleotide phosphate concentration in the region 200−600 nm using the software supplied by Jasco.

*2.9 Thermal denaturation studies*

Thermal RNA denaturation experiments were carried out with an Agilent spectrum Cary 100 spectrophotometer equipped with a Cary 100 temperature-control programmer (± 0.1°C). The temperature of the solution was increased from 25 at a rate of 1.0 °C $min^{-1}$, and the absorbance at about 260 nm was continuously monitored for solutions of RNA (32 μM) in the presence of different concentrations of each metal complex. The data were presented as $(A - A_0)/(A_f - A_0)$ vs $T$ ($T$ = temperature), where $A_f$, $A_0$, and $A$, respectively, are the final, the initial, and the observed absorbance at 260 nm. The thermal melting temperature ($T_m$) was obtained from the first derivative curve ($d\alpha/dT$) ($\alpha = (A - A_0)/(A_f - A_0)$) [7].

*2.10. Viscosity study*

The viscometric measurement was carried out with an Ubbelohde viscometer maintained at a constant temperature of (20 ± 0.1) °C in a thermostatic bath. Adding the sample solutions (10 mL) to the viscometer, then measure the flow time using a digital stopwatch, and each sample was measured three times. Relative viscosities for the triplex RNA in either in the absence or presence of metal complex was calculated according to literature procedures reported earlier [18].

## 3. Results and Discussion

*3.1. Synthesis and characterization*

Briefly, the oligopeptide ligands, pic-$Lys_2$-Gly-$Lys_2$-Gly-$Lys_2$ and pic-$Arg_2$-Gly-$Arg_2$-Gly-$Arg_2$, were synthesized using standard Fmoc chemistry starting from Rink amide resin by incorporating the pip-$CO_2H$ building block into the preassembled N-terminal (L)-peptide domains, and the Ru(II)

polypyridyl metallopeptides Ru**1** and Ru**2** were prepared in a single step reaction by treating the appropriate oligopeptide ligand with equal precursor $[Ru(bpy)_2Cl_2]$ in ethanol/water. In the Maldi-TOF-MS of either Ru**1** or Ru**2**, four molecular ion peaks are observed and the determined molecular weight is corresponding to the anticipated molecular weight of the conjugated complex. Both Ru**1** and Ru**2** give well-defined $^1$H NMR spectra, which permitted unambiguous identification and assessment of purity.

*3.2. Electronic Absorption Spectra*

The electronic absorption spectra of Ru**1** and Ru**2** in the absence of the triplex (Fig.1) are very similar to each other in phosphate buffer, displaying a IL and MLCT band at 285 and 461 nm respectively. Compared with the parent complex $[Ru(bpy)_2(pip)]^{2+}$ in the absence of the triplex [14], however, the MLCT bands of the two metallopeptides display 4-nm red shifts, suggesting that the electronic structure of the parent complex is slightly perturbed upon attachment to the peptides. Due to the different natures of Ru**1** and Ru**2**, we have anticipated that basic amino acid residues would be able to regulate the interactions of the two metallopeptides with the triplex. To evaluate the binding properties of the two metallopeptides with the triplex, a series of RNA titrations are carried out by using poly(U)•poly(A)⋆ poly(U) (Fig. 2). In all cases, no precipitation or turbidity is observed. The overall variation trends in the absorption spectra of Ru**1** and Ru**2** upon adding the triplex are very similar to one another, displaying clear hyperchromic effects upon binding with the triplex. However, the spectral changes of the two metallopeptides sharply differ from the parent complex $[Ru(bpy)_2(pip)]^{2+}$ [14],whose absorption spectra shows hypochromic effect in the presence of the triplex, suggestint that the two

metallopeptides bind toward the triplex via an electrostatic mode [19]. Binding of Ru**1** with the triplex results in a modest hyperchromic effect of *ca.* 13% at the MLCT band with no obvious red shift, while slightly smaller hyperchromicities (9%) are observed for Ru**2** at the same band. We speculate that the slight differences in hyperchromicities of Ru**1** and Ru**2** arise from the two metallopeptides containing different cationic amino acid residues. Notably, the spectral changes of Ru**1** and Ru**2** at the MLCT bands in the presence of the triplex are obviously different from what observed for the intercalating parent complex $[Ru(bpy)_2(pip)]^{2+}$ bound to the triplex (reduction of 13% in the MLCT band) [14]. Furthermore, it has been observed that small molecules which bind in the major groove of a triplex usually exhibit large spectral changes when the major groove of the template duplex is filled by the third strand [20]. No such changes were observed with either Ru**1** or Ru**2** under study here. On the other hand, the intercalators and minor groove binding reagents have similar spectral properties when bound to a triplex [21], which is consistent with observations for Ru**1** or Ru**2** if they interact with the poly(U)•poly(A)⋆ poly(U) triplex from the minor groove.

Using changes at the MLCT bands, the intrinsic binding constants ($K_b$) and binding site size ($s$) for Ru**1** are determined to be $(7.65 \pm 0.41) \times 10^6$ $M^{-1}$ and $(0.52 \pm 0.01)$, while the corresponding values for Ru**2** are $(4.57 \pm 0.52) \times 10^6$ $M^{-1}$ and $(0.97 \pm 0.01)$, respectively. The higher $K_b$ and smaller $s$ reflect a stronger binding for Ru**1** with the triplex. In addition, the binding constants for the two metallopeptides are over an order of magnitude higher than that determined for $[Ru(bpy)_2(pip)]^{2+}$ [14], demonstrating the importance of introducing basic oligopeptides into $[Ru(bpy)_2(pip)]^{2+}$. Compared with the intercalating $[Ru(bpy)_2(pip)]^{2+}$ [14], electrostatic interactions might dominate the binding of the two metallopeptides with the anionic triplex**.** On

the other hand, hydrogen bonding interactions and hydrophobic interactions between the amino acid side chains of the two metallopeptides and nucleic acid bases may also contribute to the higher association of the two metallopeptides with the triplex [22].

*3.3. Fluorescent and colorimetric studies*

The emission of Ru**1** and Ru**2** in the absence of the triplex (Fig. 3) are also very similar in phosphate buffer, with a maxima occurring at 608 nm and 7-nm blue shift in comparison with the parent complex $[Ru(bpy)_2(pip)]^{2+}$.[14] However, upon addition of the triplex the emission of the two metallopeptides (Fig. 4) initially gradually enhances and increases 2.8 times for Ru**1** at a binding ratio of 6.4 and 2.2 times for Ru**2** at a binding ratio of 4.2. Interestingly, further adding the triplex causes a quenching (reductions of 18 and 14% for Ru**1** and Ru**2** at a binding ratio of 12.9 and 24.0, respectively) in the emission intensity for the triplex−Ru**1**/Ru**2** system. In all cases, no precipitation or turbidity is observed. Finally, the emission intensity increases 2.3 and 1.9 times for Ru**1** and Ru**2** respectively, indicating a stronger association of Ru**1** with the triplex. Notably, the overall fluorescence variation trends of the two metallopeptides in the presence of the triplex sharply differ from what observed for the parent $[Ru(bpy)_2(pip)]^{2+}$ [14], whose emission gradually enhances upon adding the triplex and then reaches a maximum, while further adding the triplex its emission is not quenched, suggesting interactions of the two metallopeptides with the triplex significantly differ from the intercalating parent complex $[Ru(bpy)_2(pip)]^{2+}$ [14]. For the two metallopeptides, the initial emission enhancement is due to the localisation of chromophores within a more rigid environment in the minor groove and reduce access to quenching by solvent or $O_2$ molecules, while the subsequent luminescence quenching may be assigned to the electrostatic repulsion between the

triplexes added later and the bound ones, which causes the existing binding to become a little loose, hence increases access to quenching by solvent or $O_2$ molecules.

.

*3.4. Conformation changes of the triplex induced by complexes*

CD spectra of the RNA poly(U)•poly(A)*poly(U) triplex with either Ru**1** or Ru**2** are depicted in Fig. 5, suggesting that the overall spectral changes of the triplex in the presence of the two metallopeptides are very similar but in some way different from what observed with the parent complex $[Ru(bpy)_2(pip)]^{2+}$ [14]. Similar to the parent complex $[Ru(bpy)_2(pip)]^{2+}$, a negative change at the intrinsic negative band of 240 nm and a induced CD signal at *ca.* 292 nm is observed except that changes in the two bands are relatively more obvious in the case of both Ru**1** and Ru**2**. However, comparison of changes in the intrinsic positive band at 260 nm may be more revealing since here there are significant differences in the behaviors of the two metallopeptides and the parent complex $[Ru(bpy)_2(pip)]^{2+}$. Adding $[Ru(bpy)_2(pip)]^{2+}$ results in a obvious negative changes at 260 nm [14]. However, sharply differing from $[Ru(bpy)_2(pip)]^{2+}$, adding the two metallopeptides results in clear hyperchromic effects at this band except that changes are slightly smaller in the case of Ru**2**. Compared to the parent complex $[Ru(bpy)_2(pip)]^{2+}$ [14] and other reported intercalating Ru(II) complexes [4f,4g,8], the clear hyperchromic effects at this characteristic band may be an indication that the RNA structure is structurally perturbed by binding of the electrostatic metallopeptides, Ru**1** and Ru**2** [23]**.**

*3.5. Thermal denaturation*

Thermal melting experiments are able to determine the binding specificity of a small molecule

either with the third strand or to the template duplex of RNA triplexes [22b.24]. Thus, the triplex stabilizing effects for Ru**1** and Ru**2** are investigated by thermal melting experiments (Fig. 6), and the quantitative data are listed in Table 1. As can be seen from Fig. 6, typical thermal deaturation profile of the triplex poly(U)•poly(A)*poly(U) in the absence of metallopeptides is biphasic under the experiment conditions used in this study. The lower temperature ($T_{m1}$ = 34.6 $^{o}$C) corresponds to the triplex transformation into the Watson–Crick base pairing duplex strand plus a single strand and the higher melting temperature ($T_{m2}$, 44.1 °C) belongs to the transition of Watson–Crick base pairing duplex strand to two single strands [25]. Interestingly, binding of Ru**1** and Ru**2** results in both melting temperatures being raised to varying extents. Upon adding Ru**1** at the binding ratio of 0.12, the values of $\Delta T_{m1}$ and $\Delta T_{m2}$ of the triplex increase by 15.0 and 20.9 °C, respectively, In the case of Ru**2**, the stabilizing effect is so strong that dissociation of the triplex shows an overlapping of both melting processes, so that only a single broad transition is observed (53.6 °C) at the binding ratio of 0.08. In this case, the corresponding values of $\Delta T_{m1}$ and $\Delta T_{m2}$ are 19.0 and 9.5 °C, respectively. This indicates that, in contrary to Ru**1**, Ru**2** prefers to stabilize third-strand of the triplex to a large extent. On the other hand, the effects of the two metallopeptides stabilizing the triplex is more pronounced than those of the parent complex $[Ru(bpy)_2(pip)]^{2+}$ [14] and other stabilizers such as coralyne [4c] and $[Ru(bpy)_2(mdpz)]^{2+}$ [26]. For the parent complex $[Ru(bpy)_2(pip)]^{2+}$, it stabilizes the third strand ($\Delta T_{m1}$ = 4.1 °C) with no effect on the duplex of the triplex, reflecting the binding of this complex with the triplex is favored by third-strand to a great extent. Regarding coralyne and $[Ru(bpy)_2(mdpz)]^{2+}$, the two compounds are respectively the strongest stabilizers of small organic molecules and metal complexes reported so far. Similar to $[Ru(bpy)_2(pip)]^{2+}$, coralyne stabilized the third strand

($\Delta T_{m1}$ = 12.4 °C) of the triplex without affecting the stability of the duplex, while $\Delta T_{m1}$ and $\Delta T_{m2}$ of the triplex in the presence of $[Ru(bpy)_2(mdpz)]^{2+}$ rised by 15.6 and 7.1°C, respectively. Herein, we assume that the stronger stabilizing effects of Ru**1** and Ru**2** arises mainly from cationic amino acid residues of the two metallopeptides binding to and neutralizing phosphate groups of the triplex, which is further confirmed by viscosity experiments (Fig. 7). As seen from Fig. 7, both Ru**1** and Ru**2** have very little influence on viscosity of the riplex over the concentration range, reflecting that the two metallopeptides bind to the triplex by electrostatic interaction. On the other hand, the role of hydrogen bond formation between the two complexes and the triplex is likely to be a minor factor since previous studies on the acridine derivatives−triplex DNA binding confirmed that intermolecular hydrogen bonds does not significantly affect the stability of RNA triplexes [22a], similar behaviors are also observed for Ru(II) complexes [22b].

Furthermore, the ability to specifically stabilize the triplex by Ru**1** and Ru**2** can also be confirmed by the two metallopeptides stabilizing the template duplex poly(U)•poly(A) under the same conditions (Fig. 8, Table 2). Obviously, the arginine-rich metallopeptide, Ru**2**, is more effective in stabilizing the triplex than the lysine-rich one, and this effect may be due to the differences in the interactions of arginine and lysine with the triplex. To our knowledge, the metallopeptide Ru**2** is the most effective stabilizer compared to Ru**1** and other reported stabilizers. Such example provides evidence that a Ru(II) polypyridyl complex functionalized with hexaarginines is able to significantly increase the third-strand stabilization from 34.6 $^{o}$C up to 53.6 $^{o}$C ($\Delta T_m$ = 19.0 $^{o}$C) at a very low concentration (Ru**2** = 2.6 μM).

## 4. Conclusions

In summary, this work reports a example of two novel Ru(II) polypyridyl peptides as triplex RNA stabilizers. The obtained results suggest that attaching cationic peptides to a Ru(II) polypyridyl complex can obviously enhance the triplex stabilization. At least for the RNA sequence studied, the Arg-rich metallopeptide is slightly more effective in stabilizing the third-strand than the Lys-rich one, which may be due to the differences in interaction of arginine and lysine residues with the third strand of the triplex. Thus, this work provides a potential means to improving the triplex stabilization through decreasing interchain electrostatic repulsion by cationic amino acid residues. Future work will investigate whether changes made to RNA and the metallopeptide sequence as well as the fraction of basic amino acid residues can selectively stabilize RNA triplexes.

## Acknowledgements

This work was supported by the National Natural Science Foundation of China (21671165) .

## References

[1] (a) F.A. Buske, J.S. Mattick, T.L. Bailey, RNA Biol. 8 (2011) 427-439;

(b) A. Bacolla, G. Wang, K.M. Vasquez, PLoS Genet. 11 (2015) e1005696;

(c) G. Devi, Y. Zhou, Z.S. Zhong, D.F.K. Toh, G. Chen, WIREs RNA 6 (2015) 111-128;

(d) J.A. Brown, WIREs RNA (2020) e1598.

[2] M. Li, T. Zengeya, E. Rozners, J. Am. Chem. Soc. 132 (2010) 8676-8681.

[3] S. Das, G.S. Kumar, A. Ray, M. Maiti, J. Biomol. Struct. Dyn. 20 (2003) 703-713.

[4] (a) D.P. Arya, R.L. Coffee, I.J. Charles, J. Am. Chem. Soc. 123 (2001) 11093-11094;

(b) V.K. Tam, Q. Liu, Y. Tor, Chem. Commun. 25 (2006) 2684-2686;

(c) R. Sinha, K.G. Suresh, J. Phys. Chem. B. 113 (2009) 13410-13420;

(d) D.P. Arya, Acc. Chem. Res. 44 (2011) 134-146;

(e) L. Haque, A.B. Pradhan, S. Bhuiya, S. Das, Phys. Chem. Chem. Phys. 17 (2015) 17202-17213;

(f) L.F. Tan, J. Liu, J.L. Shen, X.H. Liu, L.L. Zeng, L.H. Jin, Inorg. Chem. 51 (2012) 4417-4419;

(g) M.N. Peng, Z.Y. Zhu, L.F. Tan, Inorg.Chem. 56 (2017) 7312-7315.

[5] H.J. Xi, E. Davis, N. Ranjan, L. Xue, D. Hyde-Volpe, D.P. Arya, Biochemistry 50 (2011) 9088-9113.

[6] A.K. Shchyolkina, E.N.Timofeev, Y.P. Lysov, V.L. Florentiev, T.M. Jovin, D.J. Arndt-Jovin, Nucleic Acids Res. 29 (2001) 986-995.

[7] B. García, J.M. Leal, V. Paiotta, R. Ruiz, F. Secco, M.J. Venturini, Phys. Chem. B. 112 (2008) 7132-7139.

[8] (a) L.F. Tan, L.J. Xie, X.N. Sun, L.L. Zeng, G. Yang, J. Inorg. Biochem. 120 (2013) 32-38;

(b) H. Zhang, X.W. Liu, X.J. He, Y. Liu, L.F. Tan, Metallomics 6 (2014) 2148-2156.

[9] T. Biver, Chem. Revie. 257 (2013) 2765-2783.

[10] D. Bouzada, I. Salvadó, G. Barka, G. Rama, J. Martínez-Costas, R. Lorca, Á. Somoza, M. Melle-Franco, M.E. Vázquez, M.V. López, Chem. Commun. 54 (2018) 658-661.

[11] I. Gamba, I. Salvado´, R.F. Brissos, P. Gamez, J. Brea, M.I. Loza, M.E.Vázquez, M. VázquezLópez, Chem. Commun. 52 (2016) 1234-1237.

[12] J.Z. Wu, B.H. Ye, L. Wang, L.N. Ji, J.Y. Zhou, R.H. Li, Z.Y. Zhou, J. Chem. Soc. Dalton. Trans. 8 (1997) 1395-1402.

[13] L.N. Ji, X.H. Zou, J.G. Liu, Coord. Chem. Rev. 216 (2001) 513-536.

[14] Z.Y. Zhu, M.N. Peng, J.W. Zhang, L.F. Tan, J. Inorg. Biochem. 169 (2017) 44-49.

[15] B.P. Sullivan, D. Salmon, T. Meyer, Inorg. Chem. 17 (1978) 3334-3341.

[16] G. Cohen, H. Eisenberg, Biopolymers 8 (1969) 45-55.

[17] M.T. Carter, M. Rodriguez, A.J. Bard, J. Am. Chem. Soc. 111 (1989) 8901-8911.

[18] (a) N.P. Vladimir, R.S. Richard, Biochemistry 37 (1998) 12952-12961;

(b) C. Lynda, D. Marc, J.F. Robert, E.K. Tia, Chem. Commun. 46 (2010) 103-105.

[19] R.J. Morgan, S. Chatterjee, A.D. Baker, T.C. Strekas, Inorg. Chem. 30 (1991) 2687-2692.

[20] (a) S.K. Kim, B. Nordén, FEBS Lett. 315 (1993) 61-64;

(b) E. Tuite, B. Nordén, Chem. Commun. 1 (1995) 53-54.

[21] E.Tuite, B. Nordén, Bioorg. Med. Chem. 3 (1995) 701-711.

[22] (a) H.K. Kim, J.M. Kim, S.K. Kim, A. Rodger, B. Nordén, Biochemistry 35 (1996) 1187-1194;

(b) S.D. Choi, M.S. Kim, S.K. Kim, P. Lincoln, E. Tuite, B. Nordén, Biochemistry 36 (1997) 214-223.

[23] S.U. Rehman, T. Sarwar, M.A. Husain, H.M. Ishqi, M. Tabish. Arch. Biochem. Biophys. 576 (2015) 49-60.

[24] W. Ni, X.H. Liu, L.F.Tan, J. Inorg. Biochem. 186 (2018) 51-59.

[25] O. Doluca, A.S. Boutorine, V.V. Filichev, Chem BioChem. 12 (2011) 2365-2374.

[26] X.J. He, J. Li, H. Zhang, L.F. Tan, Mol. BioSyst. 10 (2014) 2552-2557.

## Captions for Schemes and Figures

**Scheme 1.** Chemical structures of Ru**1** and Ru**2**. These formulae are for the fully protonated forms.

**Fig. 1.** The absorption spectra of Ru**1** ($2 \times 10^{-5}$ M) and Ru**2** ($2 \times 10^{-5}$ M) in phosphate buffer.

**Fig. 2.** Representative absorption spectral changes of Ru**1** (a) and Ru**2** (b) in the presence of the triplex in phosphate buffer (6 mmol/L $Na_2HPO_4$, 2 mmol/L $NaH_2PO_4$, 1 mmol/L $Na_2EDTA$, 19 mmol/L NaC1, pH 7.0) at 20 $^oC$. [Ru**1**] = [Ru**2**] = 20 μM. For Ru**1** and Ru**2**, [UAU] = 0-34.0 and 0-47.9 μM, respectively. Where UAU stands for the triplex. The arrows show the absorbance changes upon an increasing the triplex concentration. Inserts: plots of $(\varepsilon_a - \varepsilon_b)/(\varepsilon_f - \varepsilon_b)$ *vs*.[UAU] by nonlinear fit.

**Fig. 3.** The steady-state fluorescence spectra of Ru**1** ($2 \times 10^{-6}$ M) and Ru**2** ($2 \times 10^{-6}$ M) in phosphate buffer.

**Fig. 4.** Representative fluorescence emission spectra of Ru**1** (a) and Ru**2** (b) treated with the triplex. [Ru**1**] = [Ru**2**] = 2.0 μM, For Ru**1** and Ru**2**, [UAU] = 0-28.4 and 0-23.9 μM, respectively. The arrows show the intensity change upon an increasing the triplex concentration. Solution conditions are the same as those described in the legend of FIGURE 2.

**Fig. 5.** CD spectra of the triplex (A, 100 μM) treated with Ru**1** (a) and Ru**2** (b) at different [Ru]/[UAU] ratios from 0 to 0.21 for Ru**1** and 0 to 0.48 for Ru**2**, respectively. Solution conditions are the same as those described in the legend of FIGURE 2.

**Fig. 6.** UV melting graph of the triplex (32.0 uM) in the presence of Ru**1** (a) and Ru**2** (b). Where UAU stands for the triplex. [$Na^+$] = 35 mM. Solution conditions are the same as those described in the legend of FIGURE 2.

**Fig. 7.** Effect of the increasing concentration of Ru**1** and Ru**2** on the relative viscosity of the triplex (153 μM) in phosphate buffer at 20 °C.

**Fig. 8.** Melting curves at 260 nm of poly(A)•poly(U) (32.0 μM) and its complexation with Ru**1** (a) and Ru**2** (b) in phosphate buffer (6 mmol/L $Na_2HPO_4$, 2 mmol/L $NaH_2PO_4$, 1 mmol/L $Na_2EDTA$, 19 mmol/L NaC1, pH 7.0)

**Table 1.** $T_m$ values of the triplex in the presence of Ru**1** and Ru**2**, where UAU stands for the triplex and Ru stands Ru**1** and Ru**2**. [$Na^+$] = 35 mM.

| Title/Complex | $C_{Ru}/C_{UAU}$ | $T_{m1}$ (°C) | $T_{m2}$ (°C) | $\Delta T_{m1}$ | $\Delta T_{m2}$ |
|---|---|---|---|---|---|
| poly(U)•poly(A)*poly(U) | 0 | 34.6 | 44.1 | — | — |
| poly(U)•poly(A)*poly(U)+Ru**1** | 0.02 | 39.4 | 59.6 | 4.8 | 15.5 |
| | 0.04 | 42.6 | 59.6 | 7.6 | 15.5 |
| | 0.06 | 43.4 | 63.5 | 8.8 | 19.4 |
| | 0.08 | 47.9 | 64.1 | 13.3 | 20.0 |
| | 0.12 | 49.6 | 65.0 | 15.0 | 20.9 |
| poly(U)•poly(A)*poly(U)+Ru**2** | 0.01 | 37.9 | 50.9 | 3.3 | 6.0 |
| | 0.02 | 45.1 | 54.0 | 10.5 | 9.9 |
| | 0.04 | 46.0 | 54.0 | 11.4 | 9.9 |
| | 0.06 | 48.9 | 54.1 | 14.3 | 10.0 |
| | 0.08 | 53.6 | 53.6 | 19.0 | 9.5 |
| | 0.12 | 52.1 | 52.1 | 17.5 | 8.0 |

**Table 2.** $T_m$ values of poly(A)•poly(U) in the presence of Ru**1** and Ru**2**. Where Ru and AU stand for Ru**1**, Ru**2** and poly(A)•poly(U), respectively. [$Na^+$] = 35 mM.

| Title/Complex | $C_{Ru}/C_{UAU}$ | $T_m$ | $\Delta T_m$ |
|---|---|---|---|
| poly(A)•poly(U) | 0 | 44.1 | 0 |
| poly(A)•poly(U) + Ru**1** | 0.04 | 58.3 | 14.2 |
| | 0.12 | 63.6 | 19.5 |
| poly(A)•poly(U) + Ru**2** | 0.04 | 53.9 | 9.8 |
| | 0.12 | 52.4 | 8.4 |

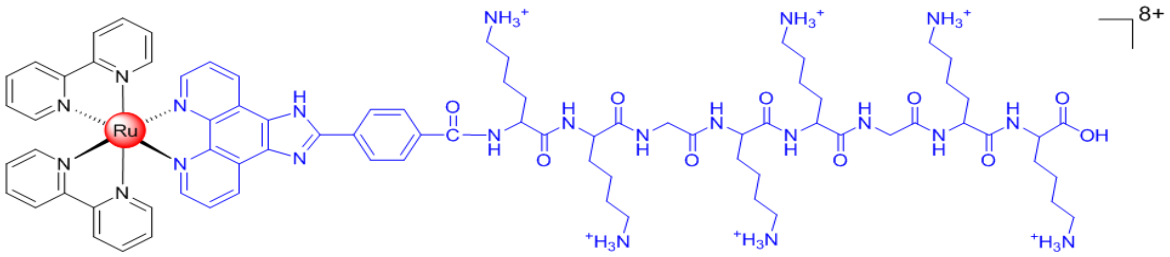


Ru**1**

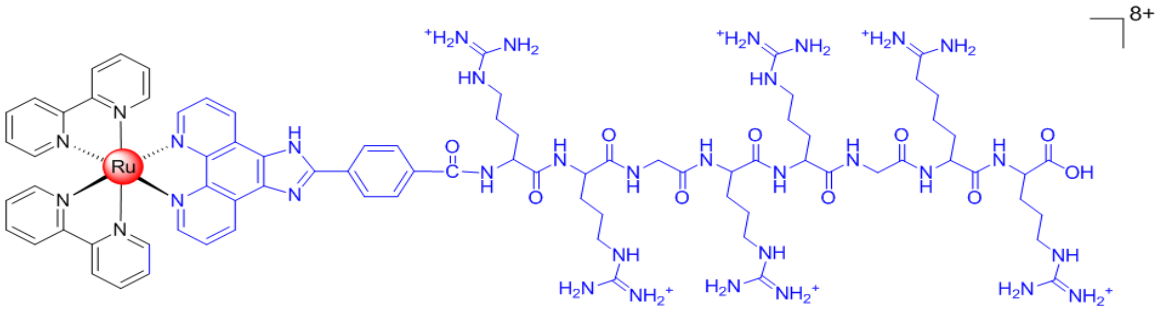


Ru**2**

**Scheme 1.**

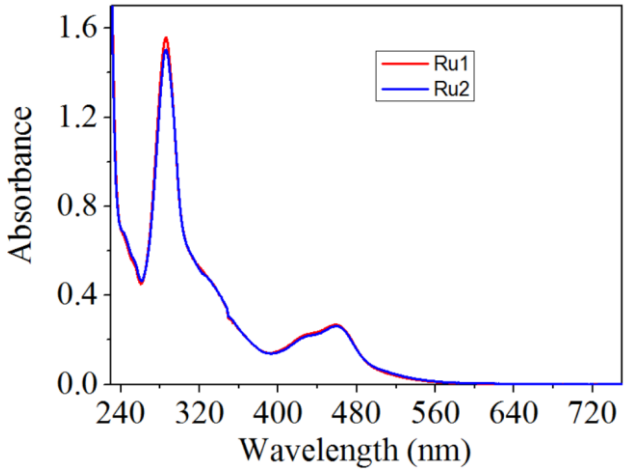


**Fig. 1.**

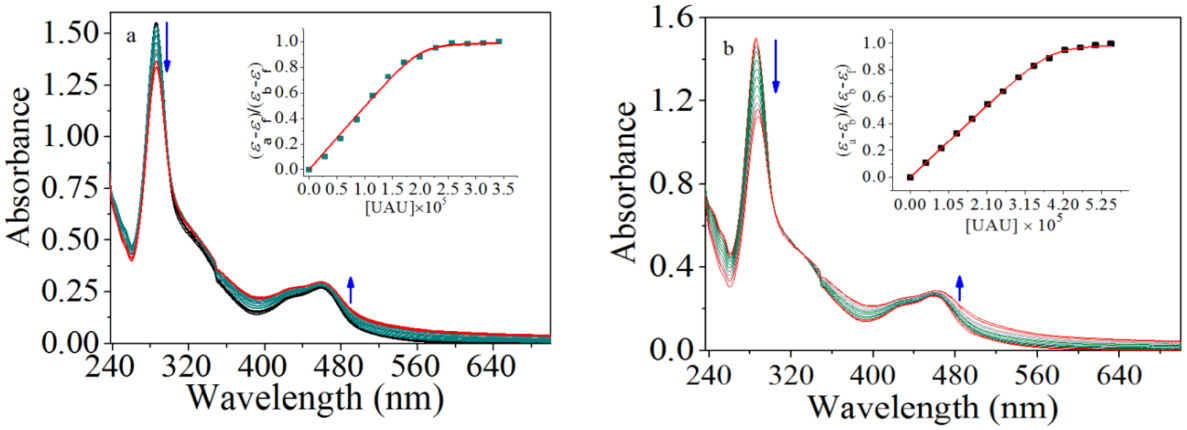


**Fig. 2.**

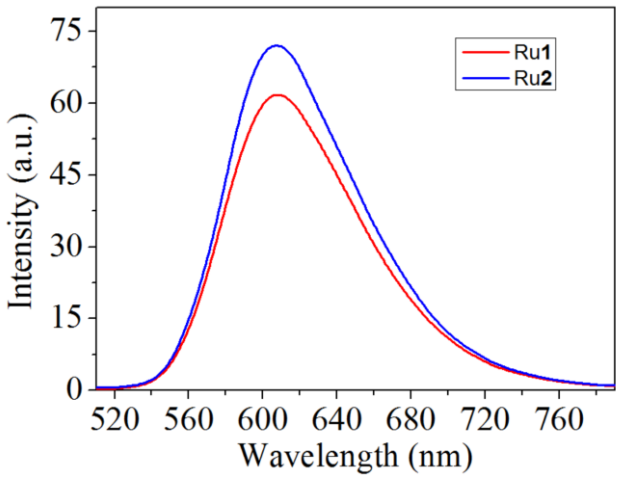


**Fig. 3.**

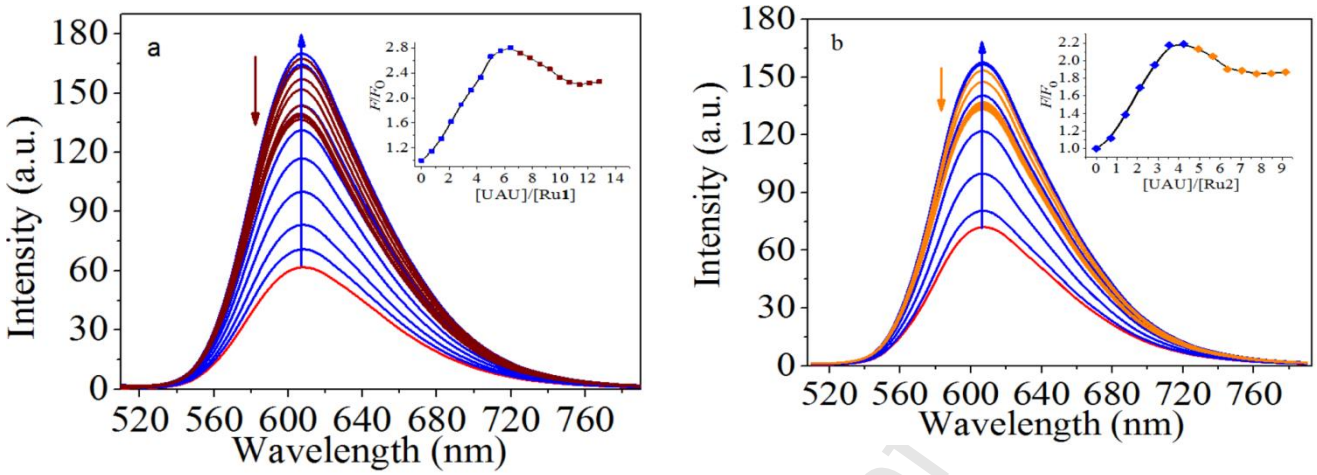


**Fig. 4.**

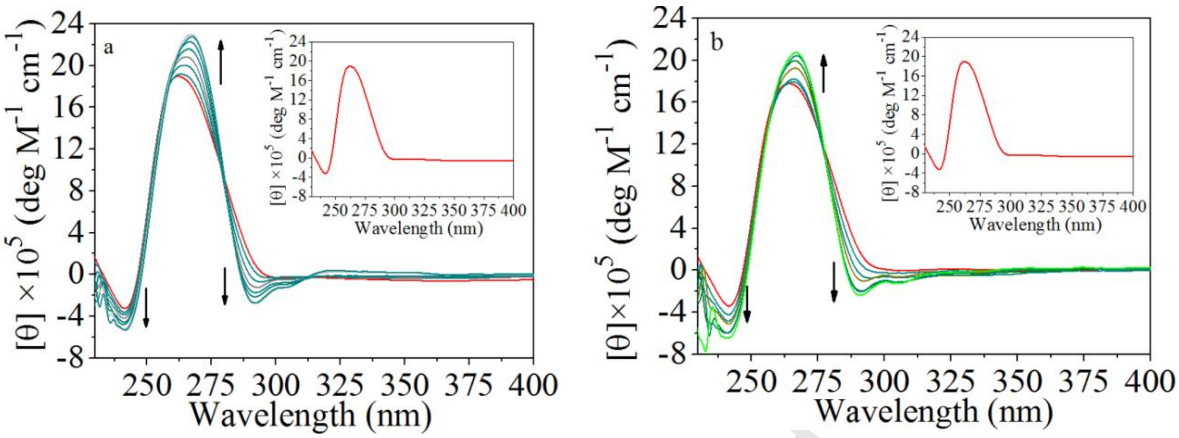


**Fig. 5.**

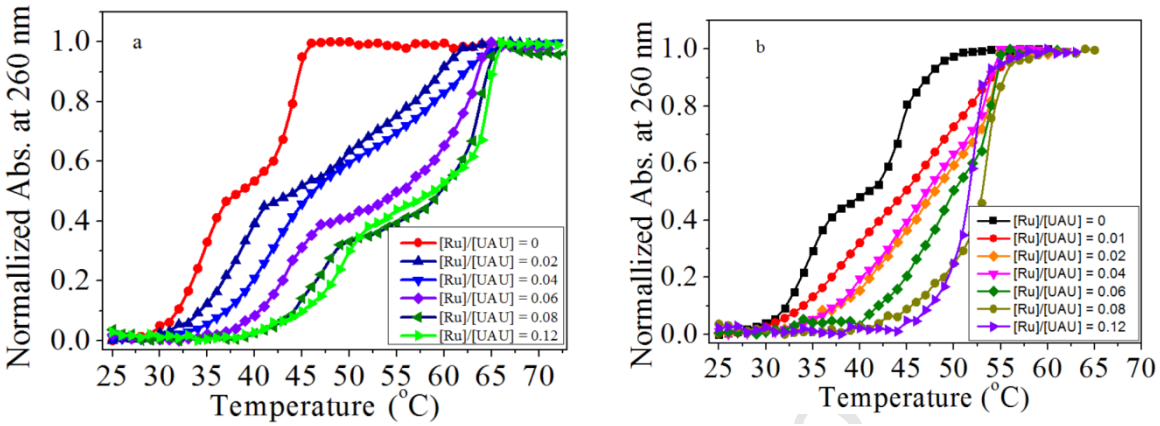


**Fig. 6.**

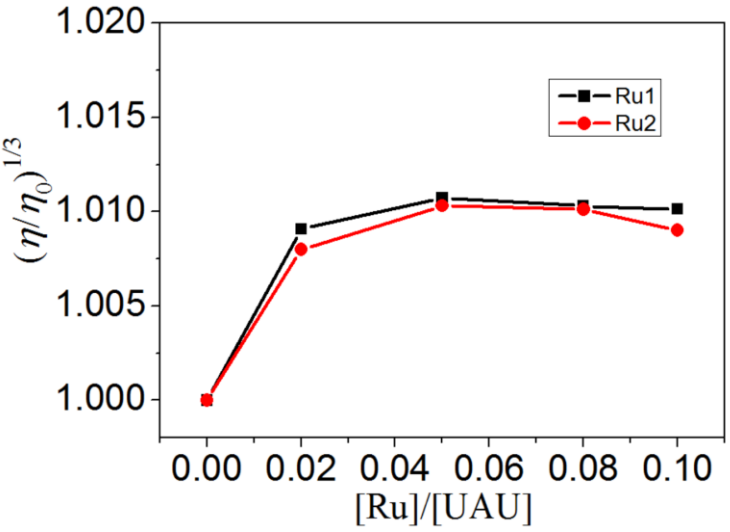


**Fig. 7.**

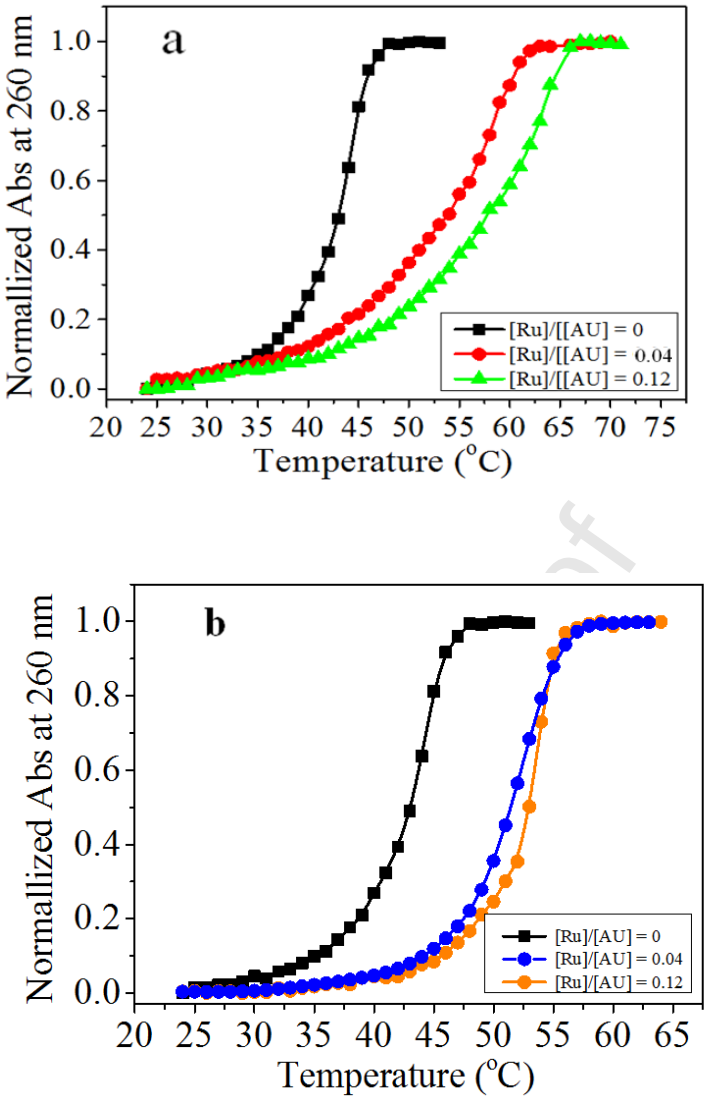
a
Normallized Abs at 260 nm
1.0
0.8
0.6
0.4
0.2
0.0
20 25 30 35 40 45 50 55 60 65 70 75
Temperature (°C)
[Ru]/[[AU] = 0
[Ru]/[[AU] = 0.04
[Ru]/[[AU] = 0.12
b
Normallized Abs at 260 nm
1.0
0.8
0.6
0.4
0.2
0.0
20 25 30 35 40 45 50 55 60 65
Temperature (°C)
[Ru]/[AU] = 0
[Ru]/[AU] = 0.04
[Ru]/[AU] = 0.12

**Fig. 8.**

## Conflict of Interest

We declare that we do not have any commercial or associative interest that represents a conflict of interest in connection with the work submitted.

**Graphical abstract**

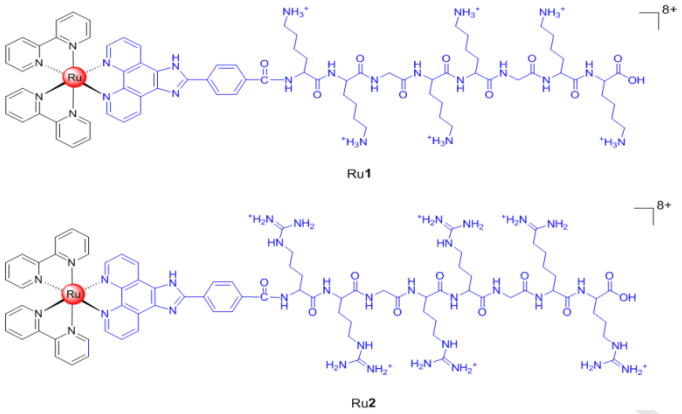


Two Lys- and Arg-rich Ru(II) polypyridyl metallopeptides Ru**1** and Ru**2** as an RNA triplex stabilizers were synthesized. Compared to Lys-rich Ru**1**, the third-strand stabilizing effect of Ru**2** is slightly more marked, which may be due to differences in the interactions of arginine and lysine residues with the triplex.

**Highlights**

- Two Arg- and Lys-rich metallopeptides Ru**1** andRu**2** were synthesized.
- Ru**1** and Ru**2** binding to an RNA triplex was investigated.
- Both complexes significantly increase the triplex stabilization.
- The third-strand stabilizating effect of Ru**2** is more marked.
- Third-strand stabilization depends on characteristics of amino acid residues.